Research Article

Modulation of A375 human melanoma cell proliferation and apoptosis by nitric oxide

Jung Hyun Kim[§]

Department of Tourism and Food Service Cuisine, Cheju Tourism College, Jeju 695-900, Republic of Korea

Seo Hyun Moon[§]

Department of Forensic DNA, National Forensic Service, Wonju, Gangwon-do 220-170, Republic of Korea

Min Young Kim* (iD)

Toxicology Laboratory, Department of Biotechnology (Biomaterials), College of Applied Life Science, Jeju National University, Jeju, 63243, Republic of Korea

[§]Contributed equally. *Corresponding author. Email: jeffmkim@jejunu.ac.kr

How to Cite

Kim, J. H. *et al.* (2022). Modulation of A375 human melanoma cell proliferation and apoptosis by nitric oxide. *Journal of Applied and Natural Science*, 14(2), 320 - 325. https://doi.org/10.31018/jans.v14i2.3365

Abstract

The present study aimed to assess the effect of NO$^{\bullet}$ on melanoma A375 cell growth and apoptotic cell death. Trypan blue exclusion assay was employed to detect the cytotoxicity induced by controlled steady-state concentrations (given in μM • min) of NO$^{\bullet}$. The characteristics of the cellular cell cycle and apoptosis in NO$^{\bullet}$-treated A375 cells were also analyzed by Annexin V/PI and DNA fragmentation assays. Western blotting was applied to detect the expression of apoptosis-related proteins (p53, Bax, Fas, DR5, caspase-3 and -9, and PARP). When exposed to preformed 100% NO$^{\bullet}$ for 8 h reactor system, a cumulative dose of 3360 μM • min reduced the viability by 22% 24 h after treatment and promoted apoptosis, 2.9- and 12.2-folds 24 and 48 h after treatment higher than the argon control, respectively. Cell cycle analysis 48 h after treatment revealed S-phase arrest in cells treated with 3360 μM • min NO$^{\bullet}$. It was also observed that the expression of p53, DR5, caspase 9 and PARP increased significantly upon NO$^{\bullet}$ treatment. In addition, the present study assessed the inhibitory effects of endogenous NO$^{\bullet}$ on the proliferation of human melanoma cells by employing specific (AMG, 1400W and/or SMTC) and nonspecific (NMA) NO$^{\bullet}$ synthase (NOS) inhibitors resulting in melanoma cell growth inhibition; the highest cytotoxic effect was seen when inducible NOS inhibition by 1 mM 1400W treatment. Collectively, the present data suggest that NO$^{\bullet}$ is involved in a key mechanism limiting melanoma proliferation and apoptosis, which may play in improving the efficacy of melanoma treatment.

Keywords: Apoptosis, Cell proliferation, Human melanoma cells, Nitric oxide

INTRODUCTION

Human melanoma is a fatal type of skin cancer and causes most skin cancer deaths. Only 20-30% of melanoma patients with visceral metastasis live beyond 5 years, and early detection with excision surgery is the sole reliable treatment of melanoma (Dind *et al*., 2021; Melo *et al*., 2021; Baldelli *et al*., 2020). Inflammation is important for maintaining homeostasis and monitoring stress signals that arise with tissue malfunction (Medzhitov, 2008). Chronic inflammation has been recognized as a driving force for epidermal cell transformation and malignant progression. Increased risk for the development of certain cancers is associated with inflammatory processes. Human melanoma is a type of tumor strongly related to inflammatory processes due to the high levels of secreted cytokines and the production of reactive oxygen species (ROS) and reactive nitrogen species (RNS). Chronic inflammatory molecules drive skin cancer development by signaling to both tumor cells and immune cells (Tang and Wang, 2016). Many clinical studies support a possible link between chronic inflammation and cancer. Tumours can develop at chronically inflamed tissues, triggered by various factors (Kim *et al*., 2021).

Nitric oxide (NO$^{\bullet}$) is a major mediator of inflammation derived from endogenous or exogenous sources (Li and Wogan, 2005). An excessive production of NO$^{\bullet}$ was related to inflammation, which can lead to increased mutations and altered enzyme and protein

function important to the multistage carcinogenesis process, while Low levels of endogenous or exogenous $NO^{\bullet}$ enhance the progression of cancer *in vitro* and *in vivo* (Li and Wogan, 2005; Miranda *et al.*, 2021). Therefore, this is complicated because it would appear to have both tumor promoting and inhibiting effects which are probably dependent on the local concentration of the molecule.

$NO^{\bullet}$ is present in various types of skin cells, including keratinocytes, melanocytes, Langerhans cells, fibroblasts and endothelial cells. Previously unknown roles for nitric oxide in dermatology continue to be uncovered. $NO^{\bullet}$ may also be pivotal during skin cancer therapy by way of mediating treatment resistance to cisplatin treatment in melanoma cells *in vitro* (Chen *et al.*, 2021; Drača *et al.*, 2021; Mazurek and Rola, 2021). Strong clinical and experimental evidence shows a correlation between the production of $NO^{\bullet}$ by tumor cells and reduced survival of patients with advanced melanoma (Dind *et al.*, 2021; Li *et al.*; 2022, Obrador *et al.*, 2021) as well as poor response to chemotherapy and radiation therapy (Skudalski *et al.*, 2022; Hanly *et al.*, 2022). However, the molecular mechanisms through which $NO^{\bullet}$ induces apoptosis in human melanoma cells or protects tumors have not been fully defined.

The purpose of the present study was to extend the above findings to determine how $NO^{\bullet}$ dose administered continuously over substantial periods affects human melanoma cell growth and apoptotic cell death. The systems used to introduce $NO^{\bullet}$ in these experiments were designed to approximate conditions of exposure physiologically relevant to chronic inflammation states.

MATERIALS AND METHODS

Cell cultures and chemicals

The human melanoma A375 cell line was selected in this study because existing evidence suggests the possible involvement of $NO^{\bullet}$ in the etiology of melanoma (Ekmekcioglu *et al.*, 2006). A375 cells were maintained in culture media composed of DMEM with 10% FBS, 2 mM L-glutamine, 100 U/mL penicillin, 100 µg/mL streptomycin. This cell line was maintained at 37 ºC in humidified 5% CO_2 atmosphere. Reagents were purchased from the following sources: cell culture materials, Lonza (Walkersville, MD); 1400W dihydrochloride, S-Methyl-L-thiocitrulline (SMTC), aminoguanidine (*AMG*) and GenElute™ mammalian genomic DNA miniprep kit, Sigma (St. Louis, MO); N^G-Monomethyl-*L-arginine*, *Monoacetate Salt* (NMA), CalBiochem (Salt Lake City, UT); $NO^{\bullet}$ assay kit, R&D Systems (Minneapolis, MN); Apoptosis detection kit, Clontech Laboratories (Palo Alto, CA); ECL™ western blotting detection reagents, GE Healthcare Bio-Sciences (Piscataway, NJ); RIPA lysis buffer and secondary goat

anti-rabbit or anti-mouse IgG conjugated to horseradish peroxidase, Santa Cruz Biotechnology (Santa Cruz, CA); anti-Bax and anti-caspase 3 antibodies, Cell Signaling Technology (Beverly, MA); anti-Fas and anti-DR5 antibodies, StressGen Biotechnologies Corp (Victoria, BC, Canada); anti-caspase 9 and PARP antibodies, BD PharMingen (San Diego, CA); and anti-p53 and anti-actin antibodies, Oncogene (Cambridge, MA). Other reagents were obtained as follows: gases from Air Gas (Edison, NJ); Silastic™ tubing (0.058 in. i.d., 0.077 in. o.d.) from Dow Corning (Midland, MI).

$NO^{\bullet}$ exposure

One day prior to treatment, A375 cells cultured at a density of 70-80% confidence were plated in 60 mm tissue culture plates to allow the cells to adhere, after which they were exposed to $NO^{\bullet}$ by diffusion through permeable Silastic™ tubing utilizing specially designed reactors, with which $NO^{\bullet}$ dose and dose-rate can be tightly controlled at steady-state concentrations described elsewhere (Kim and Kim, 2016; Kim, 2017; Kim *et al.*, 2012; Tripathi *et al.*, 2013). In this experiment, 100% $NO^{\bullet}$ was used at a steady-state concentration of 11 µM. The total $NO^{\bullet}$ dose delivered into the medium was controlled by varying the exposure time and expressed in units of µM • min: 630 µM • min (90 min); 1260 µM • min (180 min); 2520 µM • min (360 min); and 3360 µM • min (480 min). Cells exposed to argon gas under the same conditions served as negative controls.

Determination of cell viability and $NO^{\bullet}$ levels

Cell viability 24 h after treatment was determined by trypan blue exclusion. Total $NO^{\bullet}$ [nitrate (NO_3^-) plus NO_2^-] and NO_2^- production were measured with a $NO^{\bullet}$ assay kit (R&D Systems) according to manufacturer's instructions.

Detection of apoptosis

For determination of the rate of apoptosis, cells were cultured as described above and exposed to 3360 µM • min $NO^{\bullet}$, followed by 24, 48 and 72 h incubation in a humidified incubator with 5% CO_2. Cells were harvested by trypsinization centrifugation and measured by a Becton Dickinson FACScan (excitation at 488 nm) equipped with CellQuest software following annexin V-FITC and propidium iodide staining modification of a previously described protocol (Kim *et al.*, 2009).

DNA fragmentation

A375 cells were treated as above in the $NO^{\bullet}$ delivery system. For analysis of DNA fragmentation by agarose gel electrophoresis, total DNA was isolated at times 6, 12, 24 and 48 h posttreatment, using a GenElute™ mammalian genomic DNA miniprep kit as described (Kim *et al.*, 2009). DNA fragments were separated on a 1.8% (w/v) agarose gel (50 V for 2 h) and photographic

documentation was performed after staining with 0.5 ng/mL ethidium bromide.

Immunoblotting

Cells were collected from time points 12, 24 and 45 h after treatment and were lysed and the lysates were prepared using RIPA buffer with a protease inhibitor cocktail. The protein content was measured by the Bradford assay and 60 μg of total protein were separated by SDS-PAGE and transferred to polyvinylidene difluoride (PVDF) membranes (Bio-Rad). Membranes were blocked for 1-3 h in 5% w/v dried nonfat milk in TBS with 0.1% Tween-20 and incubated with primary antibodies in the blocking buffer overnight at 4 °C: anti-p53 (diluted 1:1000), anti-Bax (diluted 1:1000), anti-DR5 (diluted 1:1000), anti-Fas(CD95) (diluted 1:2000), anti-caspase 9 (diluted 1:1000), anti-caspase 3 (diluted 1:1000), anti-PARP (diluted 1:1000), and anti-actin (diluted 1:8000). The secondary reaction was performed using HRP-conjugated anti-mouse or anti-goat IgG diluted 1:8000 in the blocking buffer. As directed by the manufacturer, the immunoblots were detected using ECL. Finally, protein blots were visualized by chemiluminescence using the ChemiDoc imaging system (Bio-Rad).

Statistical analysis

Results were expressed as mean ± standard deviation (SD) of triplicate values. They were analyzed with SPSS version 12.0 (SPSS Inc. Chicago, IL, USA) using two-tailed Student's *t*-test. Significant difference was considered at $p < 0.05$ and $p < 0.01$.

RESULTS AND DISCUSSION

Effect of $NO^{\bullet}$ on cell viability

The role of $NO^{\bullet}$ in tumor progression remains unclear. $NO^{\bullet}$ has been demonstrated to promote apoptosis of cancer cells (Skudalski *et al.*, 2022; Shi *et al.*, 2022). Whereas $NO^{\bullet}$ has been demonstrated to inhibit apoptosis in a number of cell types (Özenvera and Efferth, 2020; D'Este1 *et al.*, 2020). Here the present study hypothesized that $NO^{\bullet}$ might participate in regulating melanoma survival and apoptotic death. Importantly, in

this present study, continuous $NO^{\bullet}$ and O_2 were transfered into culture media in a stirred chamber by diffusion through gas-permeable tubing, the rates of replenishment balancing the respective rates of consumption. A model to calculate $NO^{\bullet}$ and O_2 concentrations as a function of tubing lengths and delivery-gas composition have been described and reported previously (Kim *et al.*, 2012). This system has been used to quantify $NO^{\bullet}$-induced cytotoxicity and mutagenesis.

A375 cells were exposed to increasing $NO^{\bullet}$ cumulative doses from 0 to 3360 μM • min. This dose escalation was achieved by exposing cells in a reactor to a steady-state concentration of 11 μM $NO^{\bullet}$ for increasing lengths of time from 0 to 280 min. Twenty-four hours postexposure, cells showed decreased cell viability, compared with argon controls, ranging from 12% to 78% after exposure to cumulative doses of $NO^{\bullet}$ from 1260 μM • min (180 min) to 3360 μM • min (480 min), respectively (Fig. 1). Control cells with argon treatment had no effect on cell viability.

Cell cycle distribution

By FACS analysis of cell DNA content, there was an accumulation of subploid cells, sub-G1 peak (apoptotic cells), in A375 cells after treatment with $NO^{\bullet}$ (0 to 3360 μM • min) following twenty-four hours of exposure when compared with Ar-treated control group (Table 1). Exposure of $NO^{\bullet}$ resulted in a progressive and sustained accumulation of cells in the S phase, while those in the G1 and G2/M phases decreased after treatment with $NO^{\bullet}$ (Table 1). Treatment with argon, the carrier for $NO^{\bullet}$, did not affect cell survival, apoptosis, or cell cycle.

Apoptosis of A375 cells identified by flow cytometric analysis and internucleosomal DNA fragmentation

Further, annexin V staining showed that 3360 μM • min $NO^{\bullet}$ led to increased apoptosis in A375 cells (Fig. 2). Apoptosis was sharply increased 24 and 48 h after treatment; approximately 37 and 68% of cells were apoptotic 24 and 48 h after treatment with $NO^{\bullet}$ (3- and 5.5-fold over Ar control level), respectively. All increases were statistically significant ($p < 0.01$) (Fig. 2A). One of the biochemical features of apoptosis is the frag-

Table 1. Effect of steady-state NO• on cell cycle distribution in A375 cells

Total $NO^{\bullet}$ dose (μM • min)	Apoptotic cells (%) (sub-G1)	Non-apoptotic cells (%) S	G2/M
Ar	1.6 ± 0.71	12.9 ± 0.39	59.6 ± 2.19
1260	9.4 ± 2.71[**]	13.9 ± 2.41	55.6 ± 4.35
2520	12.2 ± 3.02[**]	12.9 ± 3.76	49.2 ± 3.65
3360	24.3 ± 3.12[**]	21.7 ± 0.89[**]	41.4 ± 1.03

Cellular distribution (as percentage) in different phases of the cell cycle (sub-G1, G0/G1, S and G2/M) 48 h after treatment with cumulative total dose of $NO^{\bullet}$ is represented. Results are presented as mean ± SD of three assays. [*]$p < 0.05$ and [**]$p < 0.01$ compared to Ar control by Student *t*-test.

Table 2. Cell viability, total $NO^{\bullet}$ and NO_2^{-} concentration by NOS inhibitors in A375 cells

Treatment	Viability (% control)	$NO_3^{-} + NO_2^{-}$ (µM)	NO_2^{-} (µM)
Untreated	100	21.4 ± 3.58	8.8 ± 1.24
2 mM NMA	103.2 ± 5.67	20.7 ± 1.63	8.1 ± 0.48
4 mM AMG	117.1 ± 9.70	19.0 ± 4.19	8.6 ± 2.71
1 mM 1400W	12.5 ± 1.44[**]	10.9 ± 0.13[*]	5.7 ± 0.61[*]
1 mM SMTC	77.5 ± 7.60[*]	13.1 ± 3.01[*]	7.9 ± 1.25
1 mM 1400W + 1 mM SMTC	23.9 ± 5.25[**]	11.3 ± 1.50[*]	6.4 ± 0.82

A375 cells were treated with NOS inhibitors for 48 h. Results are presented as mean ± SD of three assays. [*]$p < 0.05$ and [**]$p < 0.01$ compared to untreated control by Student *t*-test.

mentation of the genomic DNA. Therefore, we isolated the genomic DNA after treating the cells with 3360 µM • min $NO^{\bullet}$ for 6-48 h postexposure. $NO^{\bullet}$ induced a DNA ladder formation, which confirmed death by apoptosis of the melanoma treated (Fig. 2B).

Expression of apoptotic pathway-regulating proteins

As a next step, we investigated the mechanisms underlying $NO^{\bullet}$ induced cell death, focusing on apoptosis regulating proteins. For this purpose, the levels of p53, Bax, Fas, DR5, caspase 9, caspase 3 and PARP protein expression were analyzed by western blotting. Substantial increases in cellular p53, DR5, caspase 9 and PARP levels were observed 12-48 h after exposure, whereas levels of the Bax, Fas proteins were unaffected (Fig. 3). Caspase 3 protein levels were decreased 12 and 24 h after treatment, returning to control levels by 48 h (Fig. 3).

Effect of NOS inhibitors on cell proliferation

If $NO^{\bullet}$ acts as a proliferative factor in growing A375 cells, the inhibition of $NO^{\bullet}$ synthase (NOS) should de-
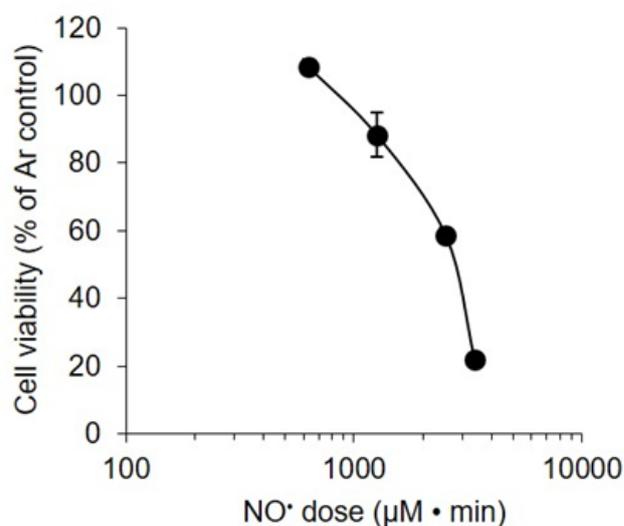
Fig. 1. *Dose−response of loss of viability following exposure of A375 cells to cumulative dose (630-3360 µM • min) of $NO^{\bullet}$. Survival was determined by a trypan blue assay 24 h after NO• treatment. Cells treated with Argon acted as negative controls. The data are represented as mean ± SD.*
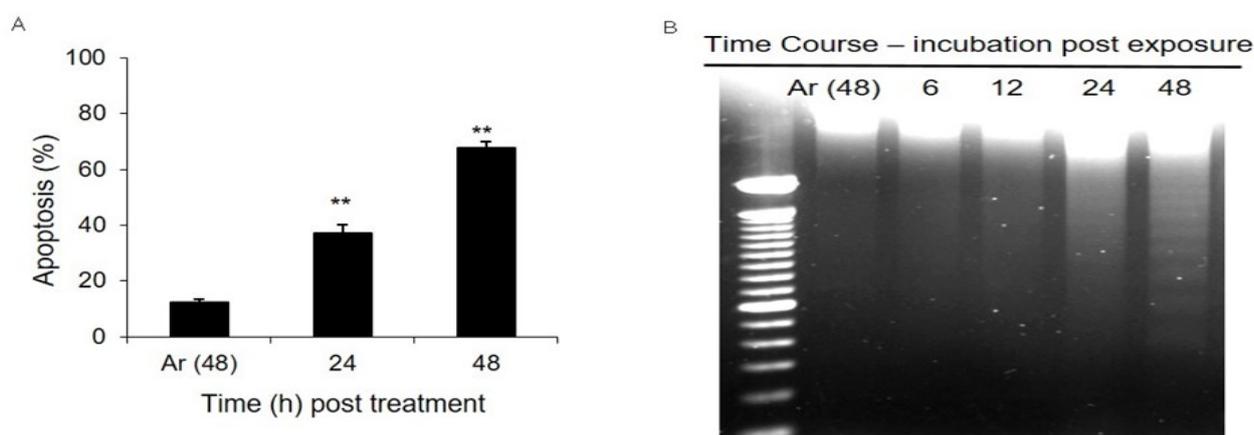
Fig. 2. *Induction of apoptosis by $NO^{\bullet}$. (A) Apoptosis was determined by annexin V versus PI staining and (B) apoptotic DNA fragmentation was detected using agarose gel electrophoresis in A375 cells treated with 3360 µM • min $NO^{\bullet}$ at 6, 12 and/or 24 and 48 h postexposure. Data shown are the mean of three independent experiments ± SD. [*]$p < 0.05$ and [**]$p < 0.01$ compared to Ar control by Student t-test.*
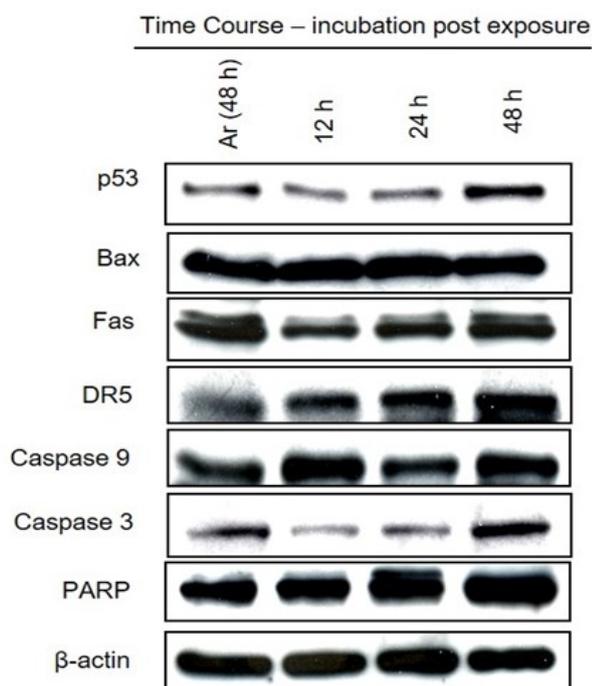
Fig. 3. *Representative Western blot showing changes on the levels of p53, Bax, Fas, DR5, caspase 9, caspase 3 and PARP. A375 cells were treated with 3360 μM • min NO˙ at 12, 24 and 48 h postexposure. Data shown are the mean of three independent experiments ± SD.*

crease cell proliferation. To assess impacts of endogenous NO˙ on the physiology of melanoma cells, growth was evaluated in cells cultured in presence of the selective iNOS inhibitor 1400 W, which resulted in marked decrease in viability (1 mM, 12.5%) in A375 cells (Table 2). A strong correlation has been shown between the prevalence of tumor cells expressing iNOS and shortened survival of patients with advanced melanoma (Liu *et al.*, 2022; Gonçalvesa *et al.*, 2019; Özenvera and Efferth, 2020; Monteiroa *et al.*, 2020). Constitutive expression of iNOS has been detected in most metastatic melanomas and melanoma cell lines (Liu *et al.*, 2022; Gonçalvesa *et al.*, 2019; Özenvera and Efferth, 2020; Monteiroa *et al.*, 2020), and it has been suggested that NO˙ contributes to tumor survival (Gonçalvesa *et al.*, 2019; Obrador *et al.*, 2021). Similar results were seen in A375 cells for nNOS inhibitor SMTC (1 mM, 77.5%), and the combination with 1400 W was more effective than SMTC alone (Table 2). Under the same experimental conditions, an iNOS inhibitor AMG (4 mM) and a nonselective NOS inhibitor NMA (2 mM) did not alter cell proliferation when compared with the untreated control (Table 2). We subsequently investigated total NO˙ and nitrite production in culture media following treatment with NOS inhibitors for 48 h. Significant levels of total NO˙ and nitrite were detected in the culture medium of A375 cells treated with NOS inhibitors (Table 2). Cells treated with 1 mM 1400W and/or 1 mM

SMTC showed 1.5- to 2-fold decreases in total NO˙ and nitrite levels compared with untreated controls ($p < 0.05$). These data suggest that the depletion of endogenous NO˙ is a prerequisite for melanoma cell growth inhibition.

Conclusion

Advances in the present understanding of melanoma would facilitate the development approval of various novel cancer therapies with NO•. The present study showed that NO• induced cell cycle arrest and apoptosis, and the depletion of endogenous NO• inhibited the growth of A375 cells. Therefore, the regulation of NO• expression may be of extreme importance in melanoma resistance to therapy. In these experiments, the systems used to introduce NO˙ in these experiments were designed to approximate exposure conditions physiologically relevant to chronic inflammation states. Further studies are required to elucidate precise mechanisms underlying these effects and their potential relevance to NO˙ induced apoptosis *in vivo*.

Conflict of interest
The authors declare that they have no conflict of interest.

REFERENCES

1. Baldelli, I., Mangialardi, M.L., Salgarello, M. & Raposio, E. (2020). Surgical reconstruction following wide local excision of malignant melanoma of the scalp. *Plastic and Reconstructive Surgery*, 8(8), e3059. doi.org/10. 1097/GOX.0000000000003059.
2. Chen, Y., Fang, L., Zhou, W., Chang, J., Zhang, X., He, C., Chen, C., Yan, R., Yan, Y., Lu, Y., Xu, C. & Xiang, C (2021) Nitric oxide-releasing micelles with intelligent targeting for enhanced anti-tumor effect of cisplatin in hypoxia. *Journal of Nanobiotechnology*, 19, 246. doi.org/10.1186/s12951-021-00989-z
3. D'Este1, F., Pietra, E.D., Pazmay, G.V.B., Xodo, L.E. & Rapozzi, V. (2020). Role of nitric oxide in the response to photooxidative stress in prostate cancer cells. *Biochemical Pharmacology*, 182, 114205. doi.org/10.1016/j.bcp.20 20.114205
4. Dind, Z., Ogata, D., Roszik, J., Qin, Y., Kim, S.H., Tetzlaff, M.T., Lazar, A.J., Davies, M.A., Ekmekcioglu, S. & Grimm, E.A. (2021). iNOS associates with poor survival in melanoma: a role for nitric oxide in the PI3K-AKT pathway stimulation and PTEN S-nitrosylation. *Frontiers in Oncolo-*

gy, 11, 631766. doi.org/10.3389/fonc.2021.631766

5. Drača, D., Edeler, D., Saoud, M., Dojčinović, B., Dunđerović, D., Đmura, g., Maksimović-Ivanić, D., Mijatović, S. & Kaluđerović, G.N. (2021). Antitumor potential of cisplatin loaded into SBA-15 mesoporous silica nanoparticles against B16F1 melanoma cells: *in vitro* and *in vivo* studies, *Journal of Inorganic Biochemistry*, 217, 111383. doi.org/10.1016/j.jinorgbio.2021.111383

6. Ekmekcioglu, S., Ellerhorst, J.A., Prieto, V.G., Johnson, M.M., Broemeling, L.D. & Grimm, E.A. (2006). Tumor iNOS predicts poor survival for stage III melanoma patients. *International Journal of Cancer*, 119, 861-866. doi.org/10.1002/ijc.21767

7. Gonçalvesa, D.A., Xistoc, R., Gonçalvesa, J.D., da Silvac, D.B., Soaresc, J.P.M., Icimotod, M.Y., Annac, C.S., Gimenezc, M., de Angelisc, K., Llesuye, S., Fernandesf, D.C., Laurindof, F., Jasiulionisa, M.G. & de Melo, F.H.M. (2019). Imbalance between nitric oxide and superoxide anion induced by uncoupled nitric oxide synthase contributes to human melanoma development, *International Journal of Biochemistry and Cell Biology*, 115, 105592. doi.org/10.1016/j.biocel.2019.105592

8. Hanly, A., Gibson, F., Nocco, S., Rogers, S., Wu, M. & Alani, R.M. (2022). Drugging the epigenome: Overcoming resistance to targeted and immunotherapies in Melanoma. *JID Innovations*, 2(2), 100090. doi.org/10.1016/j.xjidi.2021.100090

9. Kim, J.H. & Kim, M.Y. (2016) Effect of dose and dosing rate on the mutagenesis of nitric oxide in *supF* shuttle vector. *Tropical Journal of Pharmaceutical Research*, 15, 2587. doi.org/10.4314/tjpr.v15i12.8

10. Kim, M.Y. (2017) Intracellular and extracellular factors influencing the genotoxicity of nitric oxide and reactive oxygen species. *Oncology Letters*,13, 1417. doi.org/10.3892/ol.2017.5584

11. Kim, M.Y., Lim, C.H., Trudel, L.J., Deen, W.M. & Wogan, G.N. (2012) Delivery method, target gene structure, and growth properties of target cells impact mutagenic responses to reactive nitrogen and oxygen species. *Chemical Research in Toxicology*, 25, 873. doi.org/10.1021/tx2004882

12. Kim, M.Y., Trudel, L.J. & Wogan, G.N. (2009) Apoptosis induced by capsaicin and resveratrol in colon carcinoma cells requires nitric oxide production and caspase activation. *Anticancer Research*, 29, 3733-3740.

13. Kim, S.S., Sumner W.A., Miyauchi, S., Cohen, E.E.W., Califano, J.A. & Sharabi, A.B. (2021) Role of B Cells in Responses to Checkpoint Blockade Immunotherapy and Overall Survival of Cancer Patients. *Clinical Cancer Research*, 27(22), 6075-6082. doi.org/10.1158/1078-0432.CCR-21-069

14. Li, C.Q. & Wogan, G.N. (2005) Nitric oxide as a modulator of apoptosis. *Cancer Letters*, 226, 1-15. doi.org/10.1016/j.canlet.2004.10.021

15. Li, J., Sun, Y., Yan, R., Wu, X., Zou, H. & Meng, Y. (2022) Urea transporter B downregulates polyamines levels in melanoma B16 cells via p53 activation, *BBA - Molecular Cell Research, 1869*, 119236. doi.org/10.1016/j.bbamcr.2022.119236

16. Liu, R., Sun, X., Hu, Z., Peng, C. & Wu, T. (2022) Knockdown of long non-coding RNA MIR155HG suppresses melanoma cell proliferation, and deregulated MIR155HG in melanoma is associated with M1/M2 balance and macrophage infiltration. *Cells & Development*, 170, 203768. doi.org/10.1016/j.cdev.2022.203768

17. Mazurek, M. & Rola, R. (2021) The implications of nitric oxide metabolism in the treatment of glial tumors. *Neurochemistry International*, 150, 105172. doi.org/10.1016/j.neuint.2021.105172

18. Medzhitov, R. (2008) Origin and physiological roles of inflammation. *Nature*, 454(7203), 428-435. doi.org/10.1038/nature07201.

19. Melo, F.H.M. de, Gonçalves, D.A., Sousa, R.X. de, Icimoto, M.Y., Fernandes, D.C., Laurindo, F.R.M. & Jasiulionis, M.G. (2021) Metastatic Melanoma Progression Is Associated with Endothelial Nitric Oxide Synthase Uncoupling Induced by Loss of eNOS:BH4 Stoichiometry. *International Journal of Molecular Sciences*, 22(17), 9556. doi.org/10.3390/ijms22179556

20. Miranda, K.M., Ridnour, L.A., McGinity, C.L., Bhattacharyya, D. & Wink, D.A. (2021) Nitric Oxide and Cancer: When to Give and When to Take Away? *Inorganic Chemistry,* 60(21), 15941-15947. doi.org/10.1021/acs.inorgchem.1c02434

21. Monteiroa, H.P., Rodriguesb, E.G., Reisc, A.K.C.A., Longo, L.S., Ogataa, F.T., Morettie, A.I.S., da Costaa, P.E., Teodoroa, A.C.S., Toledoa, M.S., Stern, A. (2020) Nitric oxide and interactions with reactive oxygen species in the development of melanoma, breast, and colon cancer: A redox signaling perspective. *Nitric Oxide,* 89, 1-13. doi.org/10.1016/j.niox.2019.04.009

22. Obrador, E., Salvador, r., Lopez-Blanch, R., Jihad-Jebbar, A., Alcacer, J., Benlloch, M., Pellicer, J. & Estrela, J.M. (2021) Melanoma in the liver: Oxidative stress and the mechanisms of metastatic cell survival. *Seminars in Cancer Biology*, 71, 109-121. doi.org/10.1016/j.semcancer.2020.05.001

23. Özenvera, N. & Efferth, T. (2020) Small molecule inhibitors and stimulators of inducible nitric oxide synthase in cancer cells from natural origin (phytochemicals, marine compounds, antibiotics), *Biochemical Pharma*cology, 176, 113792. doi.org/10.1016/j.bcp.2020.113792

24. Shi, M., Zhang, J., Wang, Y., Peng, C., Hu, H., Qiao, M., Zhao, X. & Chen, D. (2022) Tumor-specific nitric oxide generator to amplify peroxynitrite based on highly penetrable nanoparticles for metastasis inhibition and enhanced cancer therapy. *Biomaterials*, 283, 121448.

25. Skudalski, L., Waldman, R., Kerr, P.E., & Grant-Kels, J.M. (2022) Melanoma: An update on systemic therapies. *Journal of the American Academy of Dermatology*, 86(3), 515-524. doi.org/10.1016/j.jaad.2021.09.075

26. Sun, K., Lu, X., Yin, C. & Guo, J. (2022) *In vitro* antitumor activity of nano-pulse stimulation on human anaplastic thyroid cancer cells through nitric oxide-dependent mechanisms. *Bioelectrochemistry*, 145, 108093. doi.org/10.1016/j.bioelechem.2022.108093

27. Tang, L. & Wang, K. (2016) Chronic inflammation in skin malignancies. *Journal of Molecular Signaling*, 11(2), 1-13. doi.org/10.5334/1750-2187-11-2

28. Tripathi, D.N., Chowdhury, R., Trudel, L.J., Tee, A.R., Slack, R.S., Walker, C.L. & Wogan, G.N. (2013) Reactive nitrogen species regulate autophagy through ATM-AMPK-TSC2–mediated suppression of mTORC1. *Proceedings of the National Academy of Sciences of the United States of America*, 110, E2950. doi.org/10.1073/pnas.1307736110